JPET Fast Forward. Published on February 2, 2017 as DOI: 10.1124/jpet.116.239756
This article has not been copyedited and formatted. The final version may differ from this version.

A tumor cell-selective inhibitor of mitogen-activated protein kinase phosphatases sensitizes breast cancer cells to lymphokine-activated killer cell activity

Christof T. Kaltenmeier, Laura L. Vollmer, Lawrence A. Vernetti, Lindsay Caprio, Keanu Davis, Vasiliy N. Korotchenko, Billy W. Day, Michael Tsang, Keren I. Hulkower, Michael T. Lotze, and Andreas Vogt

Author affiliations

Departments of Surgery, Immunology and Biochemistry (C.T.K., M.T.L.)

Drug Discovery Institute (L.L.V., L.A.V., L.C., K.D., M.T.L., A.V.)

Department of Computational & Systems Biology (L.A.V., A.V.)

Department of Pharmaceutical Sciences (V.N.K., B.W.D.)

Department of Developmental Biology (M.T.)

University of Pittsburgh, Pennsylvania

Platypus Technologies, LLC, Madison, WI (K.I.H.)

JPET Fast Forward. Published on February 2, 2017 as DOI: 10.1124/jpet.116.239756
This article has not been copyedited and formatted. The final version may differ from this version.

RUNNING TITLE: Selective cancer cell toxicity of MKP inhibitor

Corresponding author: Andreas Vogt, University of Pittsburgh Drug Discovery Institute, W948 Biomedical Science Tower, Pittsburgh, PA 15261, USA. Phone 412-383-5856; Fax 412-648-9009; e-mail: avogt@pitt.edu.

Text pages: 18

Tables: 0

Figures: 6

References: 51

Abstract: 245 words

Introduction, 619 words

Discussion, 1224 words

Abbreviations: BCI, (*E*)-2-benzylidene-3-(cyclohexylamino)-2,3-dihydro-1*H*-inden-1-one; DHE, dihydroethidium; DUSP, dual specificity phosphatase; EC50/IC50, half maximal effective/inhibitory concentration; FBS, fetal bovine serum; FCS, fetal calf serum; FGF, fibroblast growth factor; ERK, extracellular signal-regulated kinase; FITC, fluorescein isothiocyanate; GAL, general acid loop; HBSS, Hank's balanced salt solution; HCA, high-content analysis; hpf, hours post fertilization; LAK, lymphokine activated killer cell activity; MAPK, mitogen-activated protein kinase or MAP kinase; MKP, MAP kinase phosphatase; NK, natural killer; PI, propidium iodide; ROS, reactive oxygen species; PTP, protein tyrosine phosphatase; SAR, structure-activity relationship.

Recommended section assignment : Drug Discovery and Translational Medicine

JPET Fast Forward. Published on February 2, 2017 as DOI: 10.1124/jpet.116.239756
This article has not been copyedited and formatted. The final version may differ from this version.

ABSTRACT

Dual specificity mitogen activated protein kinase (MAPK) phosphatases (DUSP-MKPs) have been hypothesized to maintain cancer cell survival by buffering excessive MAPK signaling caused by upstream activating oncogenic products. A large and diverse body of literature suggests that genetic depletion of DUSP-MKPs can reduce tumorigenicity, suggesting that hyperactivating MAPK signaling by DUSP-MKP inhibitors could be a novel strategy to selectively affect the transformed phenotype. Through in vivo structure activity relationship studies in transgenic zebrafish we recently identified a hyperactivator of Fibroblast Growth Factor signaling (BCI-215) that is devoid of developmental toxicity and restores defective MAPK activity caused by overexpression of DUSP1 and DUSP6 in mammalian cells. Here we hypothesized that BCI-215 could selectively affect survival of transformed cells. In MDA-MB-231 human breast cancer cells, BCI-215 inhibited cell motility, caused apoptosis but not primary necrosis, and sensitized cells to lymphokine-activated killer cell (LAK) activity. Mechanistically, BCI-215 induced rapid and sustained phosphorylation of ERK, p38, and JNK in the absence of reactive oxygen species, and its toxicity was partially rescued by inhibition of p38 but not JNK or ERK. BCI-215 also hyperactivated MKK4/SEK1, suggesting activation of stress responses. Kinase phosphorylation profiling documented BCI-215 selectively activated MAPKs and their downstream substrates, but not receptor tyrosine kinases, SRC family kinases, AKT, mTOR, or DNA damage pathways. Our findings support the hypothesis that BCI-215 causes selective cancer cell cytotoxicity in part through non-redox-mediated activation of MAPK signaling, and identify an intersection with immune cell killing that is worthy of further exploration.

INTRODUCTION

Mitogen-activated protein kinase phosphatases (MKPs) are a subgroup of the dual specificity phosphatase (DUSP) family that has recently been termed DUSP-MKPs to reconcile both current gene nomenclature and historical denominations (Kidger and Keyse, 2016). DUSP-MKPs dephosphorylate and inactivate the mitogen-activated protein kinases ERK, JNK/SAPK, and p38 on tyrosine and threonine residues, thereby regulating duration and amplitude of mitogenic and survival signaling (reviewed in (Farooq and Zhou, 2004)). A large body of literature, which has been subject to several excellent reviews, supports a role of DUSP-MKPs in cancer (Keyse, 2008; Nunes-Xavier et al., 2011; Kidger and Keyse, 2016). The prototypic DUSP-MKP, DUSP1/MKP-1, is overexpressed in prostate, gastric, breast, pancreatic, ovarian, non-small cell lung (NSCLC), and metastatic colorectal cancer, and has been associated with decreased progression-free survival (Denkert et al., 2002; Montagut et al., 2010). Genetic depletion of *MKP-1* by siRNA enhances sensitivity of cancer cells to clinically used antineoplastic agents (Wu et al., 2005; Liu et al., 2014) whereas its overexpression promotes chemoresistance (Small et al., 2007). In mice, genetic ablation of *DUSP1/MKP-1* limits the tumorigenicity of pancreatic cancer cells (Liu et al., 2014) and inhibits non-small cell lung cancer tumorigenesis and metastasis (Moncho-Amor et al., 2011). Small molecule inhibitors of DUSP-MKPs could therefore provide novel approaches to treat cancer.

The discovery of potent and selective inhibitors of DUSPs has been hindered by a high degree of conservation between their active sites, a shallow and feature-poor topology (Farooq and Zhou, 2004), and the presence of a reactive, active site cysteine, which is critical for enzymatic activity but sensitive to oxidation. Perhaps not too surprisingly, *in vitro* screens for DUSP inhibitors have yielded agents that were reactive chemicals or lacked biological activity (Lazo et al., 2002; Johnston et al., 2007). The utility of DUSP-MKP inhibitors as therapeutics is also disputed because of the varied roles that DUSP-MKPs play in physiology and pathophysiology, and their overlapping substrate specificities (Farooq and Zhou, 2004). Consequently, this class of enzymes is often thought of as “undruggable”.

JPET Fast Forward. Published on February 2, 2017 as DOI: 10.1124/jpet.116.239756
This article has not been copyedited and formatted. The final version may differ from this version.

Using a zebrafish live reporter for fibroblast growth factor (FGF) activity we discovered a biologically active, allosteric inhibitor of zebrafish Dusp6/Mkp3, (*E*)-2-benzylidene-3-(cyclohexylamino)-2,3-dihydro-1*H*-inden-1-one (BCI) (Molina et al., 2009). Subsequent *in vivo* structure activity relationship (SAR) studies in zebrafish embryos coupled with mammalian cell-based assays for inhibition of DUSP1/MKP-1 and DUSP6/MKP-3 using 33 structural congeners identified an analog (BCI-215) that retained FGF hyperactivating and cellular DUSP6/MKP-3 and DUSP1/MKP-1 inhibitory activity but was non-toxic to zebrafish embryos and an endothelial cell line (Korotchenko et al., 2014). Whereas prior studies to address the question of whether DUSP-MKPs could be targeted with small molecules for cancer treatment had been limited by chemical reactivity of existing inhibitors (Vogt et al., 2005; Vogt et al., 2008), the favorable toxicity profile of BCI-215 allowed us to ask for the first time whether DUSP-MKP inhibition with small molecules could selectively affect transformed cells but spare normal cells and tissues. We found that BCI-215 inhibited survival and motility of MDA-MB-231 human breast cancer cells but did not affect viability of cultured hepatocytes. BCI-215 activated MAPK signaling pathways, caused apoptosis but not primary necrosis that was partially dependent on p38 but not ERK or JNK activity, and sensitized cells to lymphokine-activated killer (LAK) cell activity. To investigate potential mechanisms for the differential toxicity, we quantified generation of reactive oxygen species (ROS) and found that, in contrast to previously identified DUSP-MKP inhibitors, BCI-215 did not generate ROS in cancer cells, hepatocytes, or zebrafish embryos. Kinase phosphorylation arrays revealed that BCI-215 selectively activated MAPK signaling downstream of growth factor or stress receptors. The data support BCI-215 as the first cell-active inhibitor of DUSP-MKPs that causes selective cancer cell cytotoxicity and identify an intriguing intersection with immune cells that may be further exploited.

JPET Fast Forward. Published on February 2, 2017 as DOI: 10.1124/jpet.116.239756
This article has not been copyedited and formatted. The final version may differ from this version.

MATERIALS AND METHODS

Compounds and chemicals. BCI-215 (Korotchenko et al., 2014) was described previously. Sanguinarine, menadione, NSC95397, BCI, JNK-IN-8, doxorubicin, and cisplatin were from Sigma-Aldrich. CellTracker™ Green (Molecular Probes C2925), chloromethyl fluorescein diacetate, acetyl ester (CM-H_2-DCFDA, Molecular Probes C6827), Tetramethylrhodamine, ethyl ester (TMRE, Molecular Probes T-669), and dihydroethidium (DHE, Molecular Probes D1168) were from ThermoFisher. Other MAPK inhibitors were from Selleckchem (SCH772984, cat#S7101; SP600125, cat#S1460; SB203580, cat#S1076). Ficoll-Paque was from GE Healthcare Life Sciences. Interleukin 2 was a generous gift of Prometheus, Inc. The Annexin V/PI Apoptosis Detection Kit FITC was from eBioscience.

Hepatocyte mitochondrial function. Rat hepatocytes were isolated using standard two step collagenase digestion (McQueen, 1993) and sub-cultivated at 14,000 hepatocytes/well in collagen-1 coated 384 well plates in Williams E Media supplemented with 10% FBS, 2 mM L-glutamine and 50 U/ml Penicillin and streptomycin. After 4 hours medium was decanted and replaced with Hepatocyte Maintenance Media (Williams E supplemented with 1.25 mg/ml bovine serum albumin, 6.25 µg/ml human insulin, 100 nM dexamethasone, 6.25 µg/ml human transferrin, 6.25 ng/ml selenous acid, 2 mM L-glutamine, 15 mM HEPES, 100 U/mL penicillin, and 100 U/mL streptomycin). After overnight culture, cells were treated with concentration gradients of test agents. One hour after compound addition, cells were labeled with 200 nM TMRE and 4 µg/ml Hoechst 33342 for 45 min, imaged live on an ArrayScan VTI using a 10X objective, and images analyzed with the Compartmental Bioapplication. Mitochondria were identified as cytosolic spots by size and brightness. The final parameter was %HIGH_RingSpotAvgIntenCh2 (i.e., percentage of cells with TMRE puncta in the cytoplasm based on a threshold set with vehicle treated cells).

ROS generation in hepatocytes. Cells were cultured as above and labeled four hours following drug addition with 4 µM DHE for 2 hours. Hoechst 33342 was added to a 4 µg/ml final concentration during

the final hour of incubation. In the presence of ROS, DHE is oxidized to a red fluorescent dye (oxyethidium). Cells were imaged as above and the percentage of oxyethidium-nuclear positive cells calculated based on a threshold set with vehicle treated cells.

Five-day hepatocyte toxicity. A gelling solution of 1.25 mg/ml rat tail collagen type I in pH 7.2 90:10 (v/v) Williams E media/10X HBSS was overlaid onto the rat hepatocytes. The collagen gel was incubated for 1 hour at 37° C, 5% CO_2. The collagen sandwich cultures were then challenged for 5 days to test compounds in Hepatocyte Maintenance Media, without refeeding. A 10X solution of 40 µg/ml Hoechst 33342 was added during the final 2 hours of incubation followed by a 10X solution of 20 µg/ml PI for 1 hour. Cells were imaged and the percentage of PI positive cells calculated as above.

Zebrafish. All procedures involving zebrafish were reviewed and approved by the University of Pittsburgh Institutional Animal Care and Use Committee. Wildtype AB* embryos were kept in E3 medium (5 mM NaCl, 0.17 mM KCl, 0.33 mM CaCl2, 0.33 mM MgSO4). At 48 hours post fertilization (hpf), embryos were arrayed into the wells of a 96 well microplate and treated with vehicle (0.5% DMSO) or test agents. After a 30 min pre-incubation, embryos were labeled with a solution of 10 µM DHE and 40 µg/mL MS222 (tricaine methanesulfonate, Sigma) in E3 to restrict movement during imaging. Six hours after DHE loading, embryos were imaged on an ArrayScan II using a 2.5X objective. Images were analyzed for oxyethidium fluorescence with the TargetActivation Bioapplication using the MEAN_ObjectAvgIntenCh1 parameter.

Cell culture. MDA-MB-231 and BT-20 breast cancer and HeLa cervical cancer cell lines were obtained in 1997, 2013, and 2000, respectively, from the American Culture Type Collection (ATCC, Manassas, VA) and maintained as recommended. MDA-MB-231 and HeLa cells were re-authenticated in 2011 by The Research Animal Diagnostic Laboratory (RADIL) at the University of Missouri, Columbia, MO using a PCR based method that detects 9 short tandem repeat (STR) loci, followed by comparison of results to the ATCC STR database. Original ATCC stocks and re-authenticated cells were cryopreserved

JPET Fast Forward. Published on February 2, 2017 as DOI: 10.1124/jpet.116.239756
This article has not been copyedited and formatted. The final version may differ from this version.

in liquid nitrogen and maintained in culture for no more than ten passages or three months, whichever was shorter, after which cells were discarded and a new vial thawed.

HCA of apoptosis and ERK phosphorylation. MDA-MB-231 cells (10,000/well) were treated with identical concentration gradients of test agents on the right and left half of a 384 well microplate for later assessment of potential compound autofluorescence. After 24 hours, cells were fixed, permeabilized with 0.2% Triton X-100, blocked with 1% BSA/PBS, and immunostained with anti-phospho-ERK (E10, CST cat#9106L)/AlexaFluor488 and anti-cleaved caspase-3 (CST cat#9664L)/AlexaFluor594 primary/secondary antibody pairs. Plates were imaged on the ArrayScan II using a 10X 0.5NA objective. Each well was background corrected by subtracting mean phospho-ERK and cleaved caspase-3 intensities from wells that had received secondary antibody only.

Detection and quantitation of ROS in cancer cells was performed exactly as described (Vogt et al., 2008)**.** Briefly, MDA-MB-231 cells were labeled with Hoechst 33342, loaded with CM-H_2-DCFDA (5 µM, 15 min), and treated with test agents for 10 min. After two washes, cells were analyzed for Hoechst and ROS/FITC fluorescence on the ArrayScan II. Cells were classified as positive for ROS if their average FITC intensity exceeded a threshold defined as the average FITC intensity plus one SD from DMSO-treated wells.

HCA of cell motility, cytotoxicity, and colony formation in three dimensional matrigel culture are described in Supplementary Materials and Methods.

Western blotting. Western blotting was performed as described (Vogt et al., 2008). Antibodies were: pERK (T202/Y204, CST9101), total ERK (CST9102), pJNK, (T183/Y185, CST9251), total JNK, (CST9252), pp38 (T180/Y182, CST9215), total p38 (CST9212), (pMEK1/2 (S217/221, CST9121), total MEK1/2 (CST9122), pMKK4/SEK1 (S257, CST4514), MKK4/SEK1 (CST3346), GAPDH (abcam 8245). Antibodies were used at 1:1000 dilution except pJNK (1:500) and GAPDH (1:2000).

JPET Fast Forward. Published on February 2, 2017 as DOI: 10.1124/jpet.116.239756
This article has not been copyedited and formatted. The final version may differ from this version.

Phospho-kinase profiling was performed with a commercially available assay kit containing membrane-immobilized, phosphorylation-specific antibodies against forty-three human kinases spotted in duplicate (R&D Systems, Minneapolis, MN, cat# ARY003B, lot # 102609). MDA-MB-231 cells were grown to near confluency on 100 mm cell culture dishes, treated with vehicle (0.1% DMSO) or 20 μM BCI-215 for 30 min., harvested by scraping into cold PBS, pelleted at 500 x g for 3 min., and lysed in 400 μl of supplied lysis buffer. Protein content was determined by Bradford assay. Each membrane was incubated overnight at 4°C with equal amounts of lysate protein (300-400 μg) and processed as per manufacturer's instructions. Phosphorylation signals were visualized by chemiluminescence on a Fuji LAS 4000 imager, and quantified in Developer (Definiens AG, Munich, Germany) using a mapping template supplied by the manufacturer. Spot intensities were normalized to reference signals on each membrane before calculating ratios between vehicle-treated and BCI-215 treated spots.

Toxicity reversal. Cells were pre-treated (30 min for SCH772984, SP600125, SB203580, and 3 hours for JNK-IN-8) with identical concentration gradients of MAPK inhibitors on the right and left halves of a 384 well microplate. After preincubation, half of the microplate was treated with vehicle (DMSO), the other with a pro-apoptotic concentration of BCI-215 (25 μM). To eliminate potential bias through plate/edge effects, an independent plate was prepared in parallel where vehicle and BCI-215 treatments were reversed. Twenty-four hours thereafter, plates were stained with Hoechst 33342, washed once, and imaged on the ArrayScan II using a 10X objective for analysis for cell numbers and nuclear morphology. Plates were subsequently immunostained with a cleaved caspase-3/Cy5-conjugated secondary antibody pair and analyzed for apoptosis on an ArrayScan VTI using a 20X 0.75 NA objective. Four independent readouts were extracted and correlated: cell density (SelectedObjectCountPerValidField), nuclear condensation (MEAN_ObjectAvgIntenCh1), nucleus rounding (MEAN_ObjectShapeLWRCh1), and average cellular cleaved caspase-3 intensity (MEAN_AvgIntenCh2). For each parameter, data were normalized to vehicle (maximum rescue) and BCI-215 (no rescue) as % rescue = 1-((data point - DMSO)/(DMSO-BCI-215))*100.

JPET Fast Forward. Published on February 2, 2017 as DOI: 10.1124/jpet.116.239756
This article has not been copyedited and formatted. The final version may differ from this version.

Immune cell killing. Peripheral blood mononuclear cells were obtained from healthy volunteers with an established IRB approved protocol, and separated from heparinized blood on Ficoll-hypaque (GE Healthcare, Chicago) gradients as previously reported (Buchser et al., 2012). Cells were cultured in RPMI 1640 supplemented with 10% FCS, 1% glutamine, 1% penicillin/streptomycin, and stimulated with 6,000 IU of Interleukin 2 for 24 hours. After incubation, cells were washed with PBS and counted. In parallel, MDA-MB-231 cells were pretreated in a 384 well plate with vehicle or BCI-215 (3 μM). After 24 hours in culture, medium was replaced and PBMC added in two-fold serial dilutions starting with a 50-fold excess of PBMCs in triplicate. After 24 hours of co-culture, cells were fixed with formaldehyde/Hoechst 33342, washed twice with PBS, and imaged on the ArrayScan II. Cancer cells were identified by their larger nuclei compared with PBMC, setting a size gate in the DAPI channel. In experiments with chemotherapeutics, cells carrying a biosensor consisting of a mitochondrial targeting sequence derived from cytochrome c oxidase VIII linked to GFP that is a surrogate for cytochrome c release from mitochondria (Senutovitch et al., 2015) were pretreated for 24 hours with cisplatin (2 μM) or doxorubicin (400 nM), exposed to LAK as above, and cancer cells identified and quantified by green fluorescence. Cell densities were normalized to those in the absence of PBMCs. Mean cell densities from multiple independent experiments were averaged and plotted in GraphPad Prism.

Flow Cytometry. Flow cytometric analysis was performed on a C6 flow cytometer (Accuri Cytometers, Ann Arbor, MI, USA) instrument within the University of Pittsburgh Cancer Institute Flow and Imaging Cytometry core facility and analyzed using FlowJo software (Tree Star Inc, Ashland, OR, USA). Single cell suspensions were stained with Annexin/PI (eBioscience) according to the manufacturer's protocol. Cells were identified via forward and side scatter and gated accordingly. All assessments were performed immediately after 30min of incubation at 37 °C. Necrotic, early, and late apoptotic cells were defined as cells that stained positive for PI only, annexin V only, or PI and annexin V, respectively.

Statistical analysis. Multiple data points were analyzed in GraphPad Prism by one-way ANOVA using Dunnett's multiple comparison test. EC50/IC50 values were obtained from at least three independent

experiments by non-linear regression using a four parameter logistic equation. IC50, standard error, and 95% confidence intervals were calculated in GraphPad.

JPET Fast Forward. Published on February 2, 2017 as DOI: 10.1124/jpet.116.239756
This article has not been copyedited and formatted. The final version may differ from this version.

RESULTS

BCI-215 lacks oxidative toxicity to rat hepatocytes. We first extended our previous studies of developmental toxicity to a clinically relevant cell type. Freshly isolated rat hepatocytes were plated into 96 well plates and treated with two-fold concentration gradients of BCI-215, three previously described DUSP inhibitors (sanguinarine (Vogt et al., 2005), NSC95397 (Vogt et al., 2008), BCI (Molina et al., 2009), or menadione as a positive control for hepatotoxicity **(Supplemental Figure 1)**. Toxicity was assessed by a live cell, high-content assay counting propidium iodide (PI) positive cells after a 5-day exposure, and through tetramethylrhodamine ethyl ester (TMRE) staining of mitochondria, which predicts hepatotoxicity due to mitochondrial damage in the clinic with high concordance (Pereira et al., 2012). NSC95397, sanguinarine, and menadione caused cell death that correlated with loss of mitochondrial membrane integrity **(Figure 1A, B).** BCI caused cell death but did not affect mitochondrial potential. BCI-215 was completely devoid of hepatocyte toxicity up to 100 μM, suggesting low hepatic toxicity if developed into a potential therapeutic.

BCI-215 does not generate reactive oxygen species (ROS) in hepatocytes or in developing zebrafish larvae. We next quantified generation of ROS by dihydroethidium (DHE) staining. Like mitochondrial membrane potential, ROS generation is one of the best predictors of clinical hepatotoxicity (Pereira et al., 2012). From a mechanistic perspective, compounds that generate ROS can lead to non-specific, irreversible inactivation of protein tyrosine phosphatases (PTPs) and DUSPs. The active sites of all PTPs and DUSPs contain a nucleophilic cysteine that is extremely sensitive to oxidation, and while mild, reversible oxidation is a physiological mechanism to regulate activity (Seth and Rudolph, 2006), oxidation past the sulfinic acid stage is irreversible (Bova et al., 2004). Irreversible oxidation is expected for the naphthoquinone NSC95397, which generates ROS in MDA-MB-231 breast cancer cells (Vogt et al., 2008), and sanguinarine, which depletes glutathione levels (Debiton et al., 2003). We found that with the exception of BCI-215, all agents generated ROS in hepatocytes **(Figure 1C)**, providing both a mechanism for BCI-215's lack of toxicity and eliminating the possibility of nonselective oxidative

JPET Fast Forward. Published on February 2, 2017 as DOI: 10.1124/jpet.116.239756
This article has not been copyedited and formatted. The final version may differ from this version.

phosphatase inactivation. All agents that caused ROS in hepatocytes also caused ROS in zebrafish embryos, although their IC50 values were slightly different in the two models, possibly reflecting differences in compound uptake or metabolism **(Figure 1D, E).** These findings document that the cellular activities of BCI-215 in zebrafish are not mediated by nonselective oxidative processes.

BCI-215 has antimigratory and pro-apoptotic activities in breast cancer cells that correlate with induction of ERK phosphorylation. We next investigated whether BCI-215 was toxic to cancer cells. MDA-MB-231 cells were plated in an Oris™ Pro 384 cell migration plate and treated with ten-point concentration gradients of NSC95397, BCI, or BCI-215. Forty-eight hours following treatment, cells were stained live with PI and Hoechst 33342, and the percentage of PI positive cells was quantified on an ArrayScan II (ThermoFisher, Pittsburgh) high-content reader. All agents inhibited cell motility and attachment, and showed nuclear shrinkage with IC50 values between 7 and 15 μM **(Supplemental Figure 2)**. As expected for a chemically reactive structure, NSC95397 caused necrosis at antimigratory concentrations **(Supplemental Figure 2A, % PI positive cells).** Necrosis was reduced with BCI, and BCI-215 showed no signs of necrosis at antimigratory or pro-apoptotic concentrations **(Supplemental Figure 2B,C and 3A)**. BCI-215 also inhibited colony formation in the "matrigel-on-top" model, where cells are seeded at low densities, recapitulating an initial dormancy-like state followed by clonal outgrowth (Shibue et al., 2012). MDA-MB-231 cells were transduced with a mitochondrial-targeted, GFP-labeled cytochrome C biosensor (Senutovitch et al., 2015) to enable continuous live monitoring of colony growth, plated on a layer of matrigel and treated 24 hours later with various concentrations of BCI-215. Following two days of exposure, drug was removed and cells allowed to expand for an additional 4-6 days. At the end of the study, cells were incubated with PI and analyzed for cell numbers and PI positivity by high content analysis (HCA). In contrast to the short term 2D assay, BCI-215 treated cells showed pronounced cell lysis in the longer-term 3D matrigel assay **(Supplemental Figure 2D, E and 3B)**.

JPET Fast Forward. Published on February 2, 2017 as DOI: 10.1124/jpet.116.239756
This article has not been copyedited and formatted. The final version may differ from this version.

To probe mechanisms of BCI-215 induced cell death, we performed multiplexed HCA of nuclear morphology, caspase-3 cleavage (apoptosis) and ERK phosphorylation as a pharmacodynamic biomarker for DUSP-MKP inhibition. **Figure 2A** shows that BCI and BCI-215 produced shrunken, condensed nuclei that resembled pyknosis, an early apoptotic event (Elmore, 2007). Simultaneous quantitation of condensed nuclei, caspase-3 cleavage, and ERK phosphorylation revealed that both agents caused apoptosis that correlated with ERK phosphorylation **(Figure 2B).** Based on their IC50 values, BCI and BCI-215 were equipotent **(Supplemental Table 1)**; at the highest concentration tested (50 μM), however, BCI's non-specific toxicity impaired specific cellular measurements. Flow cytometric analysis confirmed apoptotic death and documented that PI positivity was a result of secondary cell membrane permeability, occurring only in Annexin V positive cells **(Figure 2C, D).**

BCI-215 sensitizes cancer cells to immune cell killing. Immune system-targeted therapies are perhaps the greatest advance in cancer treatment in the last 50 years. Despite the spectacular success with immune checkpoint inhibitors, the majority of patients do not respond (Topalian et al., 2015). Thus there is an urgent need to develop effective therapies for those patients that do not achieve durable responses, and other mechanisms of resistance should be considered including the "lymphoplegic" effects of damage associated molecular pattern (DAMP) molecule release (Lotfi et al., 2016). A promising approach to harness the immune system in the response to small molecules is immunogenic cell death (ICD) (Kroemer et al., 2013). In ICD, tumor cells undergoing apoptosis display and secrete factors that recruit immune cells to the tumor bed and enhance cell killing activity. To test whether BCI-215 might sensitize cancer cells to immune cell kill, MDA-MB-231 cells were treated with vehicle or a mildly toxic concentration of BCI-215 (3 μM) for 24 hours followed by addition of interleukin-2 (IL-2)-activated peripheral blood mononuclear cells (PBMC). After an additional 24 hour incubation, cells were fixed, stained with Hoechst 33342, and imaged on the ArrayScan II. Cancer cell nuclei were gated by their larger size compared with PBMC. **Figure 3A** shows dose-response curves of activated PBMC added to cells pretreated with vehicle or BCI-215, averaged from three separate experiments. In the presence of

JPET Fast Forward. Published on February 2, 2017 as DOI: 10.1124/jpet.116.239756
This article has not been copyedited and formatted. The final version may differ from this version.

vehicle alone, cells were relatively insensitive to immune cell kill; a maximal effect was obtained with a 20-fold excess of LAK; the EC50 was about a 10-fold excess (50,000 LAK/well). In the presence of BCI-215, the kill curve was shifted dramatically to lower numbers of PBMC, with maximal sensitization seen with as few as 1000 LAK /well, and EC50s of as few as 100 LAK/well, well over three log differences in killing. We then compared the effects of BCI-215 to two clinically used chemotherapeutic agents, doxorubicin and cisplatin, which have previously been reported to increase LAK activity in cell culture (Yamaue et al., 1991; Wennerberg et al., 2013). All agents sensitized cells to LAK activity; however BCI-215 consistently showed sensitization at lower effector ratios than cisplatin or doxorubicin **(Figure 3B).**

BCI-215 induces mitogenic and stress signaling in cancer cells without generating ROS. DUSP-MKPs have unique but overlapping substrate specificities. For example, DUSP6/MKP-3 is specific for ERK, whereas DUSP1/MKP1 dephosphorylates ERK, JNK/SAPK, and p38 (Farooq and Zhou, 2004). To establish a MAPK pathway activation profile and to corroborate the results from the immunofluorescence analysis, we performed Western blot analysis of the kinetics of p-ERK, p-JNK/SAPK, and p-p38 induction in MDA-MB-231 cells at cytotoxic concentrations of BCI and BCI-215 (20 μM). **Figure 4A** shows that both agents activated all three kinases with identical kinetics. Similar activation of signaling pathways was observed in a second TNBC line with different mutational profile and morphology (BT-20) and a non-breast cancer line (HeLa) **(Figure 4B)**. We included doxorubicin as a negative control that requires several hours for MAPK activation because of transcriptional downregulation of DUSP1/MKP-1 (Small et al., 2003). Unexpectedly, BCI-215 also activated MEK1 and MKK4/SEK1, which are upstream of ERK (Zheng and Guan, 1993) and p38/JNK, respectively (Brancho et al., 2003) **(Figure 4A, B).** While MEK1 activation was minor and not observed in all cell lines, MKK4/SEK1 phosphorylation was elevated in all three lines **(Figure 4B).** To probe if activation of MAPK signaling was a cause of nonselective oxidative stress, we analyzed MDA-MB-231 cells for generation of ROS in the presence of DUSP-MKP inhibitors. Cells were pre-labeled for 15 min. with

JPET Fast Forward. Published on February 2, 2017 as DOI: 10.1124/jpet.116.239756
This article has not been copyedited and formatted. The final version may differ from this version.

Hoechst 33342 and dichloromethyl-fluorescein diacetate, acetyl ester (CM-H2-DCFDA) as described (Vogt et al., 2008), and treated with various concentrations of NSC95397, BCI, or BCI-215. At 30 min, 1h, 2h, 3h and 5h, cells were imaged live on an ArrayScan II in the DAPI and FITC channels. **Figure 4C** shows that, as expected from our prior study (Vogt et al., 2008), the para-quinone NSC95397 generated ROS within 30 min, with an EC50 of about 3-5 μM **(Figure 4D)**. This response was diminished with BCI (EC50: 20 μM). BCI-215, at 50 μM (more than 5x the EC50 for apoptosis and p-ERK induction), did not generate ROS in MDA-MB-231 cells **(Figure 4D).** Collectively, the data indicate BCI-215 induces a stress response that is not dependent on oxidation.

Inhibition of p38, but not ERK or JNK/SAPK, partially reverses BCI-215 toxicity. We next asked whether activation of MAPK signaling contributed to BCI-215 cytotoxicity. All three MAPKs can autophosphorylate (Mingo-Sion et al., 2004; Kim et al., 2005; Morris et al., 2013), allowing us to use MAPK inhibitors to probe pathway involvement. Cells were treated on two halves of a 384 well plate with identical concentration gradients of selective ERK, JNK, and p38 inhibitors (SCH772984, JNK-IN8, and SB203580), and a multitargeted inhibitor of JNK (SP600125), respectively, bracketed around published concentrations reported to inhibit cellular MAPK activity (SCH771984, 30 nM (Morris et al., 2013); SP600125, 10 μM (Mingo-Sion et al., 2004); SB203580, 10 μM (Kim et al., 2005), and JNK-IN8, 0.5 μM (Zhang et al., 2012)). After a 30 min pre-incubation (3 hours for JNK-IN8), one half of the microplate was treated with vehicle (DMSO), the other with a pro-apoptotic concentration of BCI-215 (25 μM). After a 24 hour exposure, plates were stained with Hoechst 33342, and analyzed for cell numbers and nuclear morphology on the ArrayScan II. Plates were subsequently immunostained with a cleaved caspase-3 antibody. **Figure 5** shows that p38 and nonselective JNK inhibition partially reversed BCI-215-induced cell loss, nuclear morphology changes, and apoptosis **(Figure 5)**, whereas specific inhibition of ERK or JNK had no effect. The partial rescue of toxicity indicates that either both p38 and JNK inhibition are necessary for full reversal of toxicity, or that MAPK-unrelated pathways also contribute to BCI-215 cytotoxicity.

BCI-215 selectively activates MAPK signaling. Both the partial rescue of cellular toxicity by MAPK inhibitors and the activation of MKK4/SEK1 left open the possibility that BCI-215 caused a general stress response independent of MAPKs. To probe pathway specificity, we analyzed cellular lysates of MDA-MB-213 cells for phosphorylation of forty-three signal transduction kinases using a commercially antibody array. **Figure 6** shows that after a brief (30 minute) exposure, BCI-215 selectively activated MAPKs (p38, ERK, and JNK), as well as their downstream substrates, MSK1/2 (Deak et al., 1998) and HSP27 (Landry et al., 1992). No activation of receptor tyrosine kinases (EGFR, PDGFR), SRC family kinases, AKT, metabolic enzymes (mTOR, AMPK), DNA damage-activated pathways (p53, CHK2), or inflammatory mediators (STAT) was observed. Collectively, the results are consistent with a catalytic mechanism involving elimination of MAPK signaling negative feedback downstream of growth factor or stress receptors.

JPET Fast Forward. Published on February 2, 2017 as DOI: 10.1124/jpet.116.239756
This article has not been copyedited and formatted. The final version may differ from this version.

DISCUSSION

It has long been proposed that overexpression of DUSP-MKPs represents a dependency of cancer cells, but to date, efforts to target DUSP-MKPs with small molecules have failed. The druggability of DUSP-MKPs has been questioned based on the feature-poor nature of their catalytic site, sensitivity to oxidation, and a high degree of conservation between members of the DUSP-MKP family. It is also being argued that even if it were possible to selectively inhibit individual DUSP-MKPs, off-target effects would invariably pose a problem because of overlapping substrate specificities. Recent studies from our laboratory and findings presented in this manuscript suggest that these views may be too simplistic. BCI-215 inhibits at least two DUSPs (DUSP1/MKP-1 and DUSP6/MKP-3) and yet is completely devoid of normal cell and developmental toxicity. Because BCI-215's biological activities are not obscured by toxicity, this compound is the first to permit testing the hypothesis that it is possible to pharmacologically target DUSP-MKPs as a dependency of cancer cell survival. We found that BCI-215 selectively killed cancer cells but spared cultured hepatocytes. In contrast to previously identified DUSP-MKP inhibitors, BCI-215 did not generate ROS. BCI-215 caused apoptosis but not primary necrosis, suggesting a physiologic form of cell kill that in clinical settings might avoid the complication of tumor lysis syndrome and resultant inactivation of immune cells (Howard et al., 2011).

BCI-215 sensitized cancer cells to LAK activity. The precise molecular mechanisms for the remarkable shift in LAK potency are currently under investigation but are likely due to enhanced expression or secretion of stress ligands by treated cells, activating immune cells and causing immunogenic cell death (ICD) (Kroemer et al., 2013). The presence of immune cells in the tumor bed is one of the most powerful prognostic indicators of patient survival (Galon et al., 2006). Only a few chemotherapies induce ICD, and for those that do, better clinical outcomes have been observed (reviewed in (Kroemer et al., 2013)). ICD involves induced expression of stress ligands on tumor cells (Miyashita et al., 2015), enabling recognition of tumor cells, facilitating enhanced interactions between tumor cells and immune effectors, release of IFN gamma and HMGB1, enhanced survival/autophagy in responding cells, and lytic

JPET Fast Forward. Published on February 2, 2017 as DOI: 10.1124/jpet.116.239756
This article has not been copyedited and formatted. The final version may differ from this version.

elimination of tumor cells unable of responding temporally in an effective manner. Specific candidate mechanisms for ICD worthy of investigation are NKG2D (NK expressed molecule G2D, one of twelve 'unique' NK receptors not expressed in lymphoblastoid cell lines) or STING (for stimulator of interferon genes). Particularly innate immune cells (Feng et al., 2016) but also T-cells (Deng et al., 2014) express NKG2D as a stress receptor sensitive to stressed cells. NKG2D ligand expression is positively correlated with longer relapse-free period in breast cancer patients (de Kruijf et al., 2012). Furthermore, the mechanism of chemotherapy induced stress ligand expression likely involves the STING pathway (Woo et al., 2014) induced by DNA damage or other means to activate STING. An alternative notion is that such chemotherapy promotes immune cell attraction through enhanced recognition of 'altered self' with diminished expression of molecules in stressed cells (Fine et al., 2010).

BCI-215 sensitized cancer cells to LAK activity despite showing little cell lysis in two-dimensional culture. This could suggest that display of phosphatidylserine (Annexin V stain) and a relatively modest amount of secondary necrosis, which is necessary for soluble ligand release, are sufficient for the observed level of sensitization. Alternatively, cells grown in microenvironments that more closely resemble *in vivo* conditions might be even more susceptible to BCI-215. Experiments in long-term (one week) three-dimensional matrigel culture documented that BCI-215 prevented colony outgrowth and resulted in much higher levels of cell lysis compared to short term monolayer culture. This opens up the exciting possibility that BCI-215 could cause enhanced immunogenic cell death (ICD) in microenvironments resembling the metastatic niche.

While our LAK experiments initially focused on sensitization of cancer cells, it might also be possible to directly exploit DUSP-MKP inhibition to boost immune responses. Elevated levels of DUSP1/MKP-1 have been found in peripheral T lymphocytes in women with breast cancer (Kurt et al., 1998), possibly impairing T cell function. In aging patients, BCI enhanced the activity of T-cells by restoring defective ERK signaling caused by increased DUSP6/MKP-3 expression (Li et al., 2012). Thus it is conceivable

that BCI-215 could directly activate PBMCs or augment IL-2 activity, which is dependent on MAPK activation.

The effects of BCI and BCI-215 were not limited to MDA-MB-231 cells. BCI-215 activated MAPK signaling in BT20 and HeLa cells. BCI has been tested in the NCI 60 cell line panel (NSC150117) with a mean GI50 of 1.84 μM and a preference for leukemia cells (last tested June 2016). Consistent with this, Müschen's group demonstrated BCI selectively induced cell death in patient-derived pre-B acute lymphoblastic leukemia (pre-B-ALL) cells, likely through inhibition of DUSP6/MKP3, which they showed to be essential for oncogenic transformation in mouse models of pre B-ALL (Shojaee et al., 2015).

To what extent the effects of BCI-215 on cancer cell toxicity are mediated by DUSPs can presently not be answered definitively but the majority of results are consistent with DUSP inhibition. We know from prior studies that BCI analogs are bona fide inhibitors of at least some DUSPs. In zebrafish embryos, BCI restores FGF target gene expression in the presence of overexpressed Dusp6 but not Dusp5 or sprouty (Molina et al., 2009). BCI and BCI-215 override the effects of ectopic DUSP6/MKP-3 and DUSP1/MKP-1 expression in HeLa cells (Korotchenko et al., 2014). Thus, BCI-215 is a valuable, non-toxic chemical probe for specific DUSP-mediated biologies. In cancer cells, which express multiple, redundant DUSPs, evidence is not yet definitive but most consistent with negative feedback inhibition. BCI-215 rapidly and persistently activated MAPKs, different from the fast but transient response of growth factors or the delayed but persistent response by radiation, death ligands (Dhanasekaran and Reddy, 2008), or doxorubicin (Small et al., 2003), arguing against ligand-like or transcriptional mechanisms.

BCI-215 activated MKK4/SEK1, which is a stress-activated kinase upstream of MAPKs. This result was unexpected as SEK1 is not dephosphorylated by DUSPs but by serine/threonine phosphatases. The mechanism by which BCI-215 activates MKK4/SEK1 is currently unclear but could be interpreted as

DUSP inhibition being the trigger of cellular stress. This would be consistent with the hypothesis that DUSPs are stress-adaptive genes that allow cancer cells to tolerate the effects of oncogenic transformation, as removal of such an adaptive protection is expected to expose cells to unmitigated oncogenic signaling. An alternative explanation would be that BCI-215 has additional actions independent of DUSP inhibition and/or MAPK activation. To address this possibility, we performed phospho-kinase profiling, which documented that BCI-215 selectively activated MAPKs and their downstream substrates, but not receptor tyrosine kinases, SRC family kinases, AKT, mTOR, or metabolic, inflammatory, or DNA damage pathways. These data further support the notion that BCI-215 has specific cellular activities resulting from MAPK activation.

Whether DUSPs are the sole targets of BCI-215, and if so, whether a combination of multiple DUSPs is needed for cancer-selective cell killing and immune cell sensitization remains to be seen and will require a comprehensive analysis of BCI-215's molecular mechanism(s) of action through an array of orthogonal assays including functional genomics, target engagement studies, and chemical proteomics. We posit, however, that the unique properties of this intriguing molecule make those studies worth pursuing, not only to advance BCI-215 as a complement to cancer immunotherapy, but also to possibly uncover novel mechanisms for immunogenic cell kill.

ACKNOWLEDGMENTS

We thank Nina Senutovich for the viral stocks of the biosensor consisting of EGFP with a mitochondrial targeting sequence derived from cytochrome-C oxidase subunit VIII. We would also like to thank Drs. Herbert Zeh and Daolin Tang within the Center for Damage Associated Molecular Pattern (DAMP) Biology within the UPCI for their collegiality and insights.

AUTHORSHIP CONTRIBUTIONS

Participated in research design: Kaltenmeier, Vernetti, Day, Tsang, Lotze, and Vogt

Conducted experiments: Kaltenmeier, Vollmer, Vernetti, Caprio, Davis, Korotchenko, and Vogt

Contributed new reagents or analytic tools: Hulkower and Korotchenko

Performed data analysis: Kaltenmeier, Vernetti, Caprio, Davis, Lotze, and Vogt

Wrote or contributed to the writing of the manuscript: Kaltenmeier, Vollmer, Vernetti, Caprio, Davis, Hulkower, Day, Tsang, Lotze, and Vogt

REFERENCES

Bova MP, Mattson MN, Vasile S, Tam D, Holsinger L, Bremer M, Hui T, McMahon G, Rice A and Fukuto JM (2004) The oxidative mechanism of action of ortho-quinone inhibitors of protein-tyrosine phosphatase alpha is mediated by hydrogen peroxide. *Arch Biochem Biophys* **429**:30-41.

Brancho D, Tanaka N, Jaeschke A, Ventura JJ, Kelkar N, Tanaka Y, Kyuuma M, Takeshita T, Flavell RA and Davis RJ (2003) Mechanism of p38 MAP kinase activation in vivo. *Genes Dev* **17**:1969-1978.

Buchser WJ, Laskow TC, Pavlik PJ, Lin HM and Lotze MT (2012) Cell-mediated autophagy promotes cancer cell survival. *Cancer Res* **72**:2970-2979.

de Kruijf EM, Sajet A, van Nes JG, Putter H, Smit VT, Eagle RA, Jafferji I, Trowsdale J, Liefers GJ, van de Velde CJ and Kuppen PJ (2012) NKG2D ligand tumor expression and association with clinical outcome in early breast cancer patients: an observational study. *BMC Cancer* **12**:24.

Deak M, Clifton AD, Lucocq LM and Alessi DR (1998) Mitogen- and stress-activated protein kinase-1 (MSK1) is directly activated by MAPK and SAPK2/p38, and may mediate activation of CREB. *EMBO J* **17**:4426-4441.

Debiton E, Madelmont JC, Legault J and Barthomeuf C (2003) Sanguinarine-induced apoptosis is associated with an early and severe cellular glutathione depletion. *Cancer Chemotherapy & Pharmacology* **51**:474-482.

Deng L, Liang H, Xu M, Yang X, Burnette B, Arina A, Li XD, Mauceri H, Beckett M, Darga T, Huang X, Gajewski TF, Chen ZJ, Fu YX and Weichselbaum RR (2014) STING-Dependent Cytosolic DNA Sensing Promotes Radiation-Induced Type I Interferon-Dependent Antitumor Immunity in Immunogenic Tumors. *Immunity* **41**:843-852.

Denkert C, Schmitt WD, Berger S, Reles A, Pest S, Siegert A, Lichtenegger W, Dietel M and Hauptmann S (2002) Expression of mitogen-activated protein kinase phosphatase-1 (MKP-1) in primary human ovarian carcinoma. *International Journal of Cancer* **102**:507-513.

Dhanasekaran DN and Reddy EP (2008) JNK signaling in apoptosis. *Oncogene* **27**:6245-6251.

Elmore S (2007) Apoptosis: a review of programmed cell death. *Toxicol Pathol* **35**:495-516.

Farooq A and Zhou MM (2004) Structure and regulation of MAPK phosphatases. *Cell Signal* **16**:769-779.

Feng H, Dong Y, Wu J, Qiao Y, Zhu G, Jin H, Cui J, Li W, Liu YJ, Chen J and Song Y (2016) Epirubicin pretreatment enhances NK cell-mediated cytotoxicity against breast cancer cells in vitro. *Am J Transl Res* **8**:473-484.

Fine JH, Chen P, Mesci A, Allan DS, Gasser S, Raulet DH and Carlyle JR (2010) Chemotherapy-induced genotoxic stress promotes sensitivity to natural killer cell cytotoxicity by enabling missing-self recognition. *Cancer Res* **70**:7102-7113.

Galon J, Costes A, Sanchez-Cabo F, Kirilovsky A, Mlecnik B, Lagorce-Pages C, Tosolini M, Camus M, Berger A, Wind P, Zinzindohoue F, Bruneval P, Cugnenc PH, Trajanoski Z, Fridman WH and Pages F (2006) Type, density, and location of immune cells within human colorectal tumors predict clinical outcome. *Science* **313**:1960-1964.

Howard SC, Jones DP and Pui C-H (2011) The Tumor Lysis Syndrome. *The New England Journal of Medicine* **364**:1844-1854.

Johnston PA, Foster CA, Shun TY, Skoko JJ, Shinde S, Wipf P and Lazo JS (2007) Development and implementation of a 384-well homogeneous fluorescence intensity high-throughput screening assay to identify mitogen-activated protein kinase phosphatase-1 dual-specificity protein phosphatase inhibitors. *Assay Drug Dev Technol* **5**:319-332.

Keyse SM (2008) Dual-specificity MAP kinase phosphatases (MKPs) and cancer. *Cancer Metast Rev* **27**:253-261.

Kidger AM and Keyse SM (2016) The regulation of oncogenic Ras/ERK signalling by dual-specificity mitogen activated protein kinase phosphatases (MKPs). *Semin Cell Dev Biol* **50**:125-132.

Kim L, Del Rio L, Butcher BA, Mogensen TH, Paludan SR, Flavell RA and Denkers EY (2005) p38 MAPK autophosphorylation drives macrophage IL-12 production during intracellular infection. *J Immunol* **174**:4178-4184.

Korotchenko VN, Saydmohammed M, Vollmer LL, Bakan A, Sheetz K, Debiec KT, Greene KA, Agliori CS, Bahar I, Day BW, Vogt A and Tsang M (2014) In vivo structure-activity relationship studies support allosteric targeting of a dual specificity phosphatase. *Chembiochem* **15**:1436-1445.

Kroemer G, Galluzzi L, Kepp O and Zitvogel L (2013) Immunogenic cell death in cancer therapy. *Annu Rev Immunol* **31**:51-72.

Kurt RA, Urba WJ, Smith JW and Schoof DD (1998) Peripheral T lymphocytes from women with breast cancer exhibit abnormal protein expression of several signaling molecules. *Int J Cancer* **78**:16-20.

Landry J, Lambert H, Zhou M, Lavoie JN, Hickey E, Weber LA and Anderson CW (1992) Human HSP27 is phosphorylated at serines 78 and 82 by heat shock and mitogen-activated kinases that recognize the same amino acid motif as S6 kinase II. *J Biol Chem* **267**:794-803.

Lazo JS, Nemoto K, Pestell KE, Cooley K, Southwick EC, Mitchell DA, Furey W, Gussio R, Zaharevitz DW, Joo B and Wipf P (2002) Identification of a potent and selective pharmacophore for Cdc25 dual specificity phosphatase inhibitors. *Mol Pharmacol* **61**:720-728.

Li G, Yu M, Lee WW, Tsang M, Krishnan E, Weyand CM and Goronzy JJ (2012) Decline in miR-181a expression with age impairs T cell receptor sensitivity by increasing DUSP6 activity. *Nat Med* **18**:1518-1524.

Liu F, Gore AJ, Wilson JL and Korc M (2014) DUSP1 is a novel target for enhancing pancreatic cancer cell sensitivity to gemcitabine. *PLoS One* **9**:e84982.

Lotfi R, Kaltenmeier C, Lotze MT and Bergmann C (2016) Until Death Do Us Part: Necrosis and Oxidation Promote the Tumor Microenvironment. *Transfus Med Hemother* **43**:120-132.

McQueen CA (1993) Isolation and culture of hepatocytes from different laboratory species, in *Methods in toxicology* (Tyson CA and Frazier JM eds) pp 255-261, Academic Press, San Diego.

Mingo-Sion AM, Marietta PM, Koller E, Wolf DM and Van Den Berg CL (2004) Inhibition of JNK reduces G2/M transit independent of p53, leading to endoreduplication, decreased proliferation, and apoptosis in breast cancer cells. *Oncogene* **23**:596-604.

Miyashita T, Miki K, Kamigaki T, Makino I, Nakagawara H, Tajima H, Takamura H, Kitagawa H, Fushida S, Ahmed AK, Duncan MD, Harmon JW and Ohta T (2015) Low-dose gemcitabine induces major histocompatibility complex class I-related chain A/B expression and enhances an antitumor innate immune response in pancreatic cancer. *Clinical and Experimental Medicine*:1-13.

Molina G, Vogt A, Bakan A, Dai W, de Oliveira PQ, Znosko W, Smithgall TE, Bahar I, Lazo JS, Day BW and Tsang M (2009) Zebrafish chemical screening reveals an inhibitor of Dusp6 that expands cardiac cell lineages. *Nat Chem Biol* **6**:680-687.

Moncho-Amor V, Ibanez de Caceres I, Bandres E, Martinez-Poveda B, Orgaz JL, Sanchez-Perez I, Zazo S, Rovira A, Albanell J, Jimenez B, Rojo F, Belda-Iniesta C, Garcia-Foncillas J and Perona R (2011) DUSP1/MKP1 promotes angiogenesis, invasion and metastasis in non-small-cell lung cancer. *Oncogene* **30**:668-678.

Montagut C, Iglesias M, Arumi M, Bellosillo B, Gallen M, Martinez-Fernandez A, Martinez-Aviles L, Canadas I, Dalmases A, Moragon E, Lema L, Serrano S, Rovira A, Rojo F, Bellmunt J and Albanell J (2010) Mitogen-activated protein kinase phosphatase-1 (MKP-1) impairs the response to anti-epidermal growth factor receptor (EGFR) antibody cetuximab in metastatic colorectal cancer patients. *Br J Cancer* **102**:1137-1144.

Morris EJ, Jha S, Restaino CR, Dayananth P, Zhu H, Cooper A, Carr D, Deng Y, Jin W, Black S, Long B, Liu J, Dinunzio E, Windsor W, Zhang R, Zhao S, Angagaw MH, Pinheiro EM, Desai J, Xiao L, Shipps G, Hruza A, Wang J, Kelly J, Paliwal S, Gao X, Babu BS, Zhu L, Daublain P, Zhang L, Lutterbach BA, Pelletier MR, Philippar U, Siliphaivanh P, Witter D, Kirschmeier P, Bishop WR, Hicklin D, Gilliland DG, Jayaraman L, Zawel L, Fawell S and Samatar AA (2013) Discovery of a

novel ERK inhibitor with activity in models of acquired resistance to BRAF and MEK inhibitors. *Cancer Discov* **3**:742-750.

Nunes-Xavier C, Roma-Mateo C, Rios P, Tarrega C, Cejudo-Marin R, Tabernero L and Pulido R (2011) Dual-specificity MAP kinase phosphatases as targets of cancer treatment. *Anticancer Agents Med Chem* **11**:109-132.

Pereira CV, Nadanaciva S, Oliveira PJ and Will Y (2012) The contribution of oxidative stress to drug-induced organ toxicity and its detection in vitro and in vivo. *Expert Opin Drug Metab Toxicol* **8**:219-237.

Senutovitch N, Vernetti L, Boltz R, DeBiasio R, Gough A and Taylor DL (2015) Fluorescent protein biosensors applied to microphysiological systems. *Exp Biol Med (Maywood)* **240**:795-808.

Seth D and Rudolph J (2006) Redox regulation of MAP kinase phosphatase 3. *Biochemistry* **45**:8476-8487.

Shibue T, Brooks MW, Inan MF, Reinhardt F and Weinberg RA (2012) The outgrowth of micrometastases is enabled by the formation of filopodium-like protrusions. *Cancer Discov* **2**:706-721.

Shojaee S, Caeser R, Buchner M, Park E, Swaminathan S, Hurtz C, Geng H, Chan LN, Klemm L, Hofmann WK, Qiu YH, Zhang N, Coombes KR, Paietta E, Molkentin J, Koeffler HP, Willman CL, Hunger SP, Melnick A, Kornblau SM and Muschen M (2015) Erk Negative Feedback Control Enables Pre-B Cell Transformation and Represents a Therapeutic Target in Acute Lymphoblastic Leukemia. *Cancer Cell* **28**:114-128.

Small GW, Shi YY, Higgins LS and Orlowski RZ (2007) Mitogen-activated protein kinase phosphatase-1 is a mediator of breast cancer chemoresistance. *Cancer Res* **67**:4459-4466.

Small GW, Somasundaram S, Moore DT, Shi YY and Orlowski RZ (2003) Repression of mitogen-activated protein kinase (MAPK) phosphatase-1 by anthracyclines contributes to their antiapoptotic activation of p44/42-MAPK. *J Pharmacol Exp Ther* **307**:861-869.

Topalian SL, Drake CG and Pardoll DM (2015) Immune checkpoint blockade: a common denominator approach to cancer therapy. *Cancer Cell* **27**:450-461.

Vogt A, McDonald PR, Tamewitz A, Sikorski RP, Wipf P, Skoko JJ, 3rd and Lazo JS (2008) A cell-active inhibitor of mitogen-activated protein kinase phosphatases restores paclitaxel-induced apoptosis in dexamethasone-protected cancer cells. *Mol Cancer Ther* **7**:330-340.

Vogt A, Tamewitz A, Skoko J, Sikorski RP, Giuliano KA and Lazo JS (2005) The benzo (c) phenanthridine alkaloid, sanguinarine, is a selective, cell-active inhibitor of mitogen-activated protein kinase phosphatase-1. *J Biol Chem* **280**:19078-19086.

Wennerberg E, Sarhan D, Carlsten M, Kaminskyy VO, D'Arcy P, Zhivotovsky B, Childs R and Lundqvist A (2013) Doxorubicin sensitizes human tumor cells to NK cell- and T-cell-mediated killing by augmented TRAIL receptor signaling. *Int J Cancer* **133**:1643-1652.

Woo SR, Fuertes MB, Corrales L, Spranger S, Furdyna MJ, Leung MY, Duggan R, Wang Y, Barber GN, Fitzgerald KA, Alegre ML and Gajewski TF (2014) STING-dependent cytosolic DNA sensing mediates innate immune recognition of immunogenic tumors. *Immunity* **41**:830-842.

Wu W, Pew T, Zou M, Pang D and Conzen SD (2005) Glucocorticoid receptor-induced MAPK phosphatase-1 (MKP-1) expression inhibits paclitaxel-associated MAPK activation and contributes to breast cancer cell survival. *J Biol Chem* **280**:4117-4124.

Yamaue H, Tanimura H, Noguchi K, Iwahashi M, Tsunoda T, Tani M, Tamai M, Hotta T, Mizobata S and Arii K (1991) Cisplatin treatment renders tumor cells more susceptible to attack by lymphokine-activated killer cells. *J Clin Lab Immunol* **35**:165-170.

Zhang T, Inesta-Vaquera F, Niepel M, Zhang J, Ficarro SB, Machleidt T, Xie T, Marto JA, Kim N, Sim T, Laughlin JD, Park H, LoGrasso PV, Patricelli M, Nomanbhoy TK, Sorger PK, Alessi DR and Gray NS (2012) Discovery of potent and selective covalent inhibitors of JNK. *Chem Biol* **19**:140-154.

Zheng CF and Guan KL (1993) Cloning and characterization of two distinct human extracellular signal-regulated kinase activator kinases, MEK1 and MEK2. *J Biol Chem* **268**:11435-11439.

FOOTNOTES

Financial support: This project was supported in part by the National Institutes of Health National Cancer Institute [Grants CA147985, CA181450], the Kennedy Shriver National Institute of Child Health and Human Development [Grant HD053287]; and DARPA-BAA-14-14; DARPA Big Mechanism Proposal; AIMCancer: Automated Integration of Mechanisms in Cancer [Award number W911NF-14-1-0422]. K. Davis was supported on the Doris Duke Foundation Academy for Clinical Research, University of Pittsburgh (M.T. Lotze). This project used the UPCI Chemical Biology and Flow and Imaging Cytometry Core Facilities that are supported in part by award P30CA047904.

[1] Part of this work was presented at the 2014 AACR annual meeting. Vollmer L, Vernetti L, Bakan A, Korotchenko V, Bahar I, Day B, Tsang M, Vogt A. Abstract 745: A non-redox reactive allosteric inhibitor of MAPK phosphatases with selective toxicity to human cancer cells. Cancer Res. 2014;74(19 Supplement):745.

[2] Present addresses. Vasiliy N. Korotchenko: Walter Reed Army Institute of Research, Silver Spring, Maryland; Keren I. Hulkower: College of American Pathologists, Northfield, IL

FIGURE LEGENDS

Figure 1. BCI-215 is non-toxic to rat hepatocytes and developing zebrafish embryos. A-C. Rat hepatocytes were treated in 96 well plates with ten-point concentration gradients of DUSP inhibitors and menadione as a positive control for hepatotoxicity. Sanguinarine, NSC95397, BCI, and menadione, but not BCI-215 produced dose-dependent cell death in rat hepatocytes as measured by **(A)** propidium iodide (PI) uptake and **(B)** loss of mitochondrial membrane integrity. **(C)** Hepatocyte toxicity correlated with production of reactive oxygen species (ROS). **(D) and (E)** In contrast to other DUSP inhibitors, BCI-215 did not generate ROS in developing zebrafish embryos. Data and images are from a single experiment that has been repeated once. Scale bar, 500 µm.

Figure 2. BCI and BCI-215 cause apoptotic cell death at concentrations that induce ERK phosphorylation. MDA-MB-231 cells were treated with vehicle (DMSO), BCI, or BCI-215 and stained with Hoechst 33342 and anti-phospho-ERK and anti-cleaved caspase-3 antibodies, respectively. **(A)** Fluorescence micrographs show pyknotic nuclei indicative of early apoptosis. Images are maximum projections of a ten plane, 0.25 µm each z-series acquired using a 60X objective on a Molecular Devices ImageXpress Ultra high content reader. BCI and BCI-215 were at 22 µM. Scale bar, 30 µm. **(B)** Multiparametric analysis of chromatin condensation, caspase-3 cleavage, and ERK phosphorylation by high-content analysis. Each box plot is the aggregate of four (caspase) or five (nuclear condensation and ERK phosphorylation) independent experiments. Boxes show upper and lower quartiles; whiskers, range; dot, mean. *, $p<0.05$; **, $p<0.01$; ****, $p<0.001$ vs. DMSO by one-way ANOVA with Dunnett's multiple comparison test. The last data point for cleaved caspase is an n=3 for 50 µM BCI-215 with two of the three values being identical. **(C and D)** Confirmation of apoptosis with secondary cell lysis by flow cytometry. Data in **(D)** are the averages ± SEM of three independent flow cytometry experiments. Early apoptosis, Q3, Annexin V positive and PI negative; late apoptosis, Q2, Annexin V and PI positive; necrosis, Q1, PI positive, Annexin V negative.

Figure 3. BCI-215 sensitizes breast cancer cells to immune cell kill. **(A)** MDA-MB-231 cells were treated overnight in 384 well plates with vehicle or 3 μM BCI-215 followed by washout. Cells were subsequently exposed to various ratios of PBMC-derived LAK. After 24 hours, cells were fixed and stained with Hoechst 33342. Cells were imaged on the ArrayScan II, cancer cell nuclei identified and gated by their larger size compared with PBMC, and enumerated. Cell densities were normalized to vehicle or BCI-215 in the absence of activated immune cells, respectively. Data are the averages ± SEM from four independent experiments, each performed in triplicate. **(B)** Comparison of BCI-215 vs. clinically used antineoplastic agents, doxorubicin (DOX) and cisplatin (CDDP). MDA-MB-231 cells were either stained with CellTracker green or transduced with a mitochondrial-targeted, GFP-labeled cytochrome C biosensor, and processed and analyzed as in (A) except that cancer cells were specifically identified by green fluorescence instead of nucleus size gating. Each data point represents the mean ± SEM of three independent experiments, each performed in triplicate.

Figure 4. BCI-215 activates mitogen- and stress-activated protein kinase cascades in the absence of oxidative stress. (A) Activation kinetics. MDA-MB-231 human breast cancer cells were treated with BCI or BCI-215 (20 μM) for the indicated time points and analyzed for phosphorylation of the DUSP1/MKP-1 and DUSP6/MKP-3 substrates, ERK, JNK/SAPK, and p38, as well as their upstream activators MEK1 and MKK4/SEK1 by Western blot. **(B)** Activation of kinase cascades in three different cell lines. Cells were treated for 1 hour with vehicle (DMSO) 20 μM BCI-215 (215), or 5 μM doxorubicin (DOX). Data in (A) and (B) are from a single experiment that has been repeated once. **(C and D)** ROS generation. MDA-MB-231 cells were pre-labeled with Hoechst 33342 and chloromethyl-fluorescein diacetate, acetyl ester (CM-H2-DCFDA) for 30 min followed by treatment with test agents for up to 5 hours. **(C)** At the indicated time points, cells were imaged and the percentage of ROS positive enumerated. **(D)** Concentration response at the 2 hour time point. Each data point is the mean of four wells ± SEM from a single experiment that has been repeated twice.

Figure 5. Effect of MAPK inhibition of BCI-215 toxicity. MDA-MB-231 cells were pretreated with concentration gradients of MAPK inhibitors followed by vehicle or a pro-apoptotic concentration of BCI-215 (25 μM). After 24 hours, cells were stained with Hoechst 33342 and an antibody against cleaved caspase-3, and analyzed for **(A)** cell density, **(B and C)** nuclear morphology, and **(D)** caspase cleavage. Data on graphs depict % rescue from BCI, calculated as 1-((data point - DMSO)/(DMSO-BCI-215))*100. Images in **(E)** illustrate cell loss and nuclear morphology with vehicle (DMSO) and BCI-215 alone, or of BCI-215 in the presence of SCH771984 (375 nM), SB203580 (18 μM), SP600125 (18 μM), or JNK-IN8 (1.8 μM). Data are the averages of 4 – 7 independent experiments ± SEM, each performed in quadruplicate. Images are from an ArrayScan VTI using a 20X objective. Scale bar, 30 μm.

Figure 6. Phospho-kinase profiling of BCI-215 in MDA-MB-231 cells. Lysates from cells treated with vehicle (0.1% DMSO) or BCI-215 (20 μM) for 30 minutes were analyzed for phosphorylation levels of forty-three human kinases. Bar graph shows mean ± range of two independent repeats; insert shows correlation of two independent replicate runs.

JPET Fast Forward. Published on February 2, 2017 as DOI: 10.1124/jpet.116.239756
This article has not been copyedited and formatted. The final version may differ from this version.

FIGURES

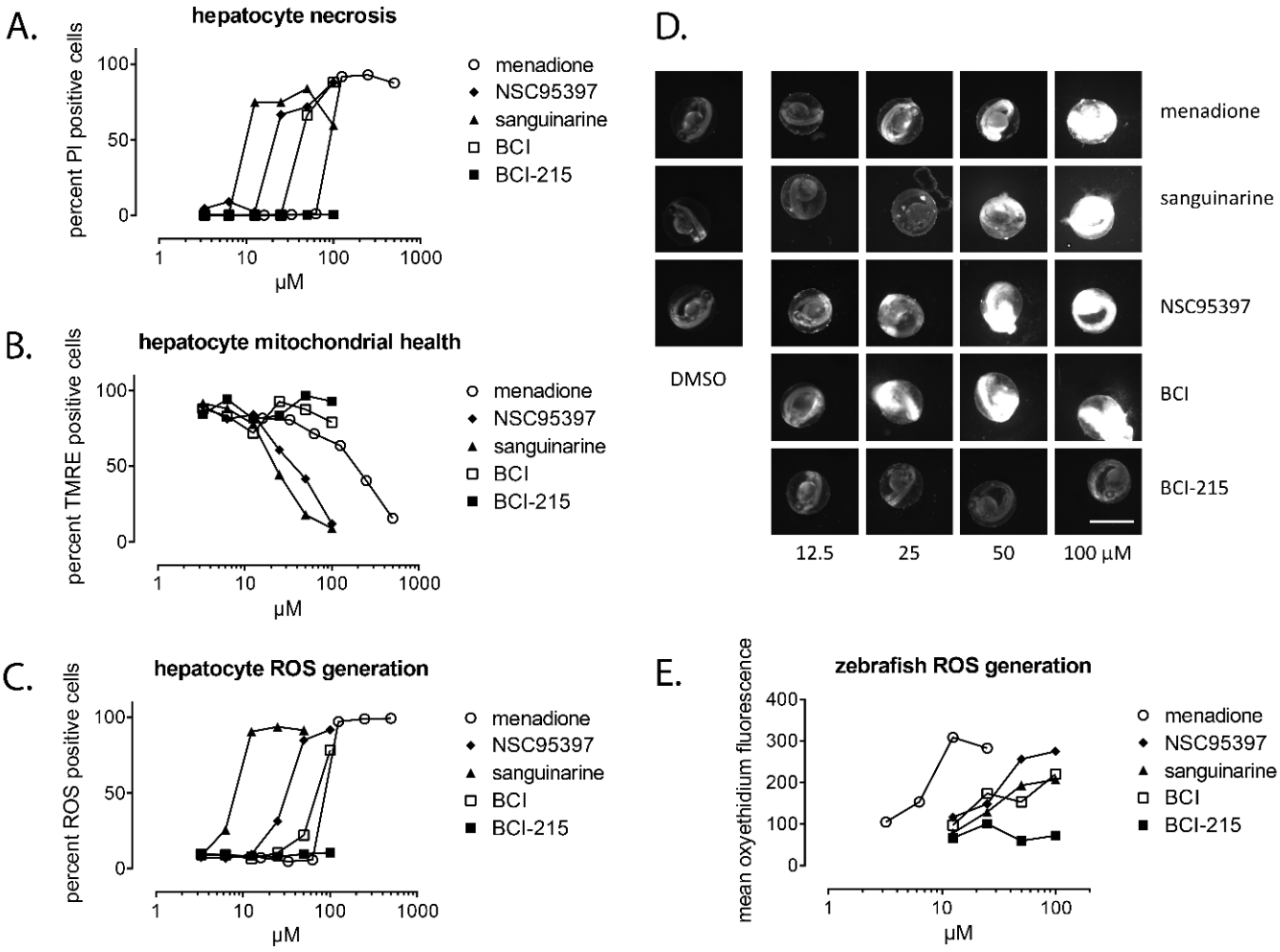

Figure 1

JPET Fast Forward. Published on February 2, 2017 as DOI: 10.1124/jpet.116.239756
This article has not been copyedited and formatted. The final version may differ from this version.

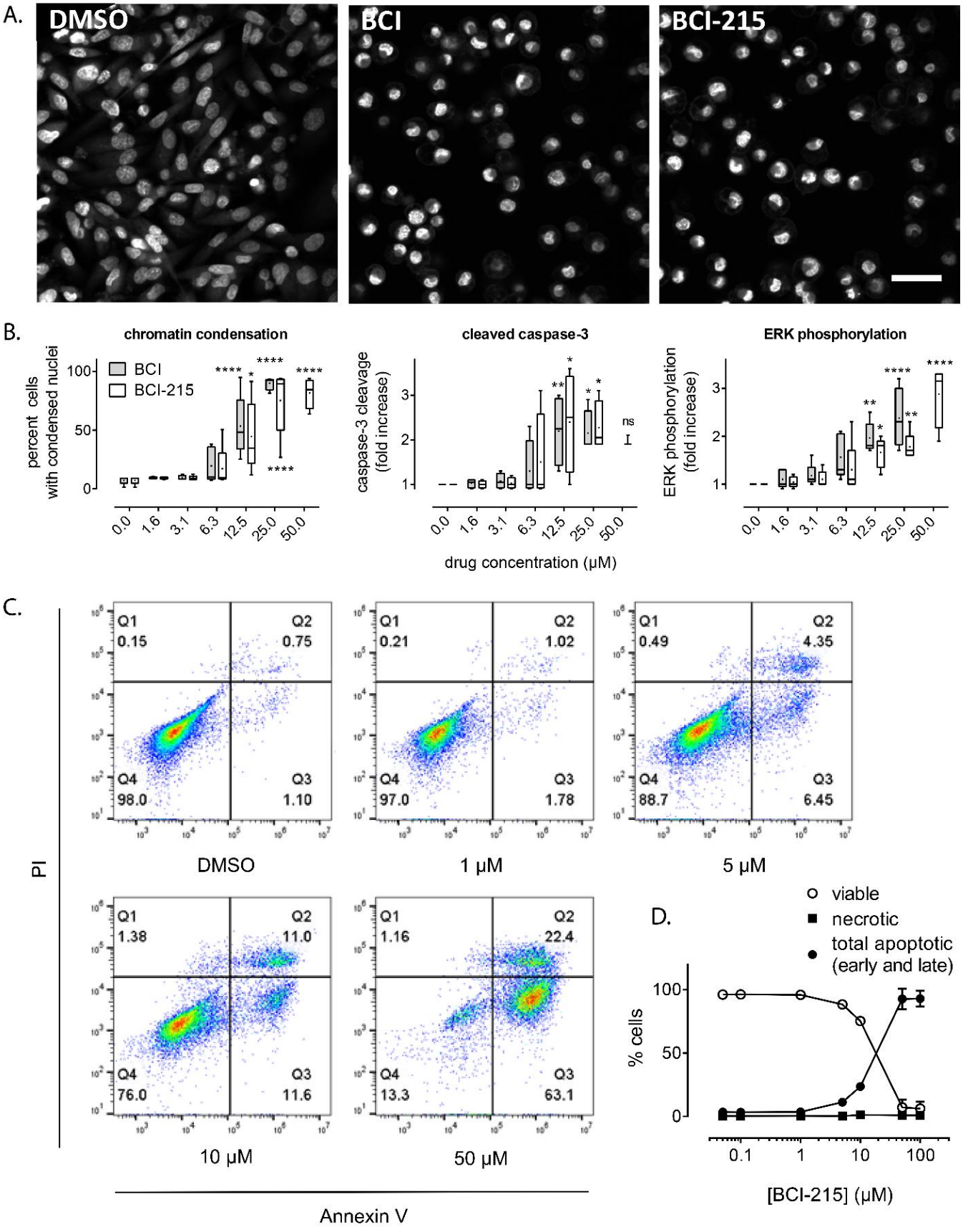

Figure 2

JPET Fast Forward. Published on February 2, 2017 as DOI: 10.1124/jpet.116.239756
This article has not been copyedited and formatted. The final version may differ from this version.

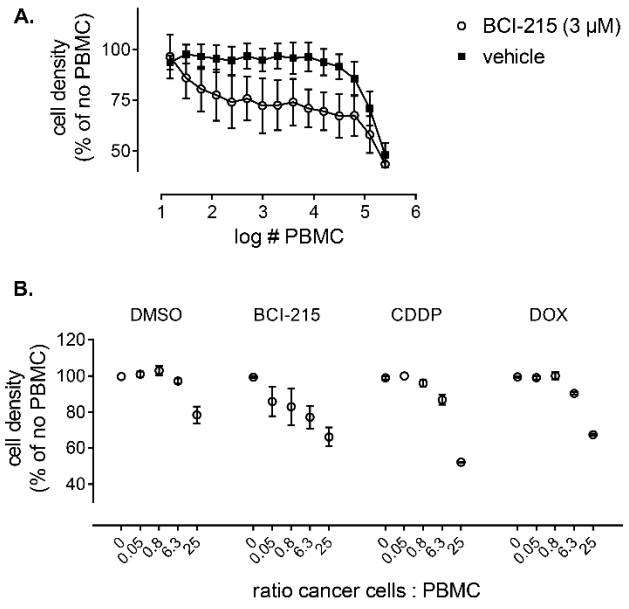

Figure 3

JPET Fast Forward. Published on February 2, 2017 as DOI: 10.1124/jpet.116.239756
This article has not been copyedited and formatted. The final version may differ from this version.

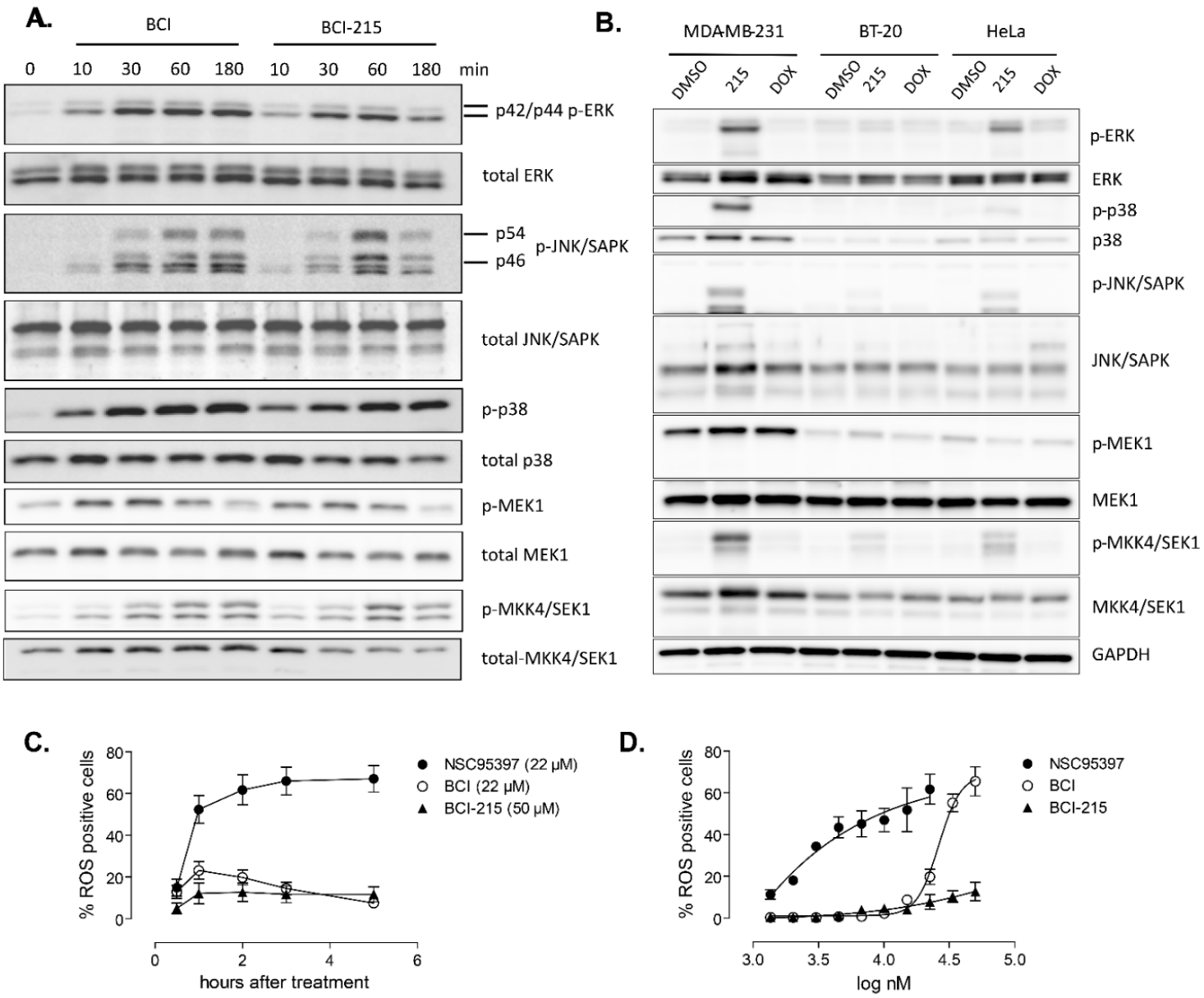

Figure 4

JPET Fast Forward. Published on February 2, 2017 as DOI: 10.1124/jpet.116.239756
This article has not been copyedited and formatted. The final version may differ from this version.

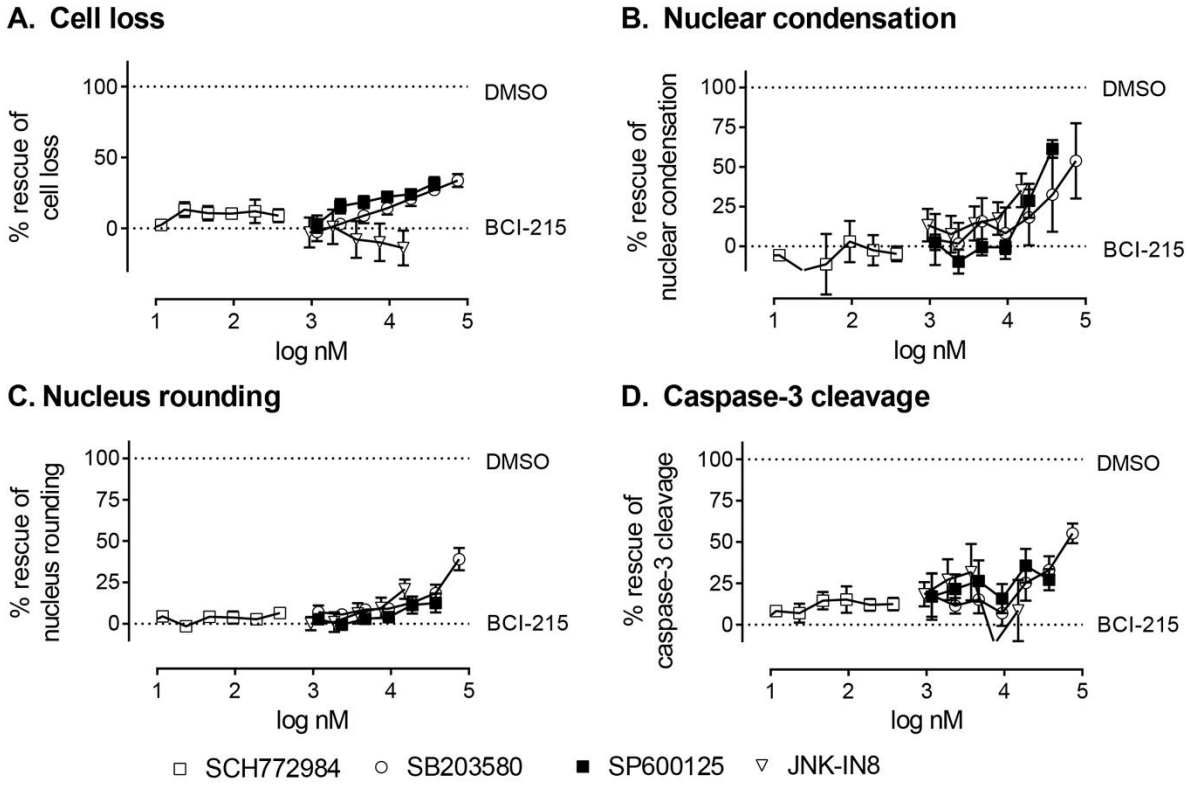

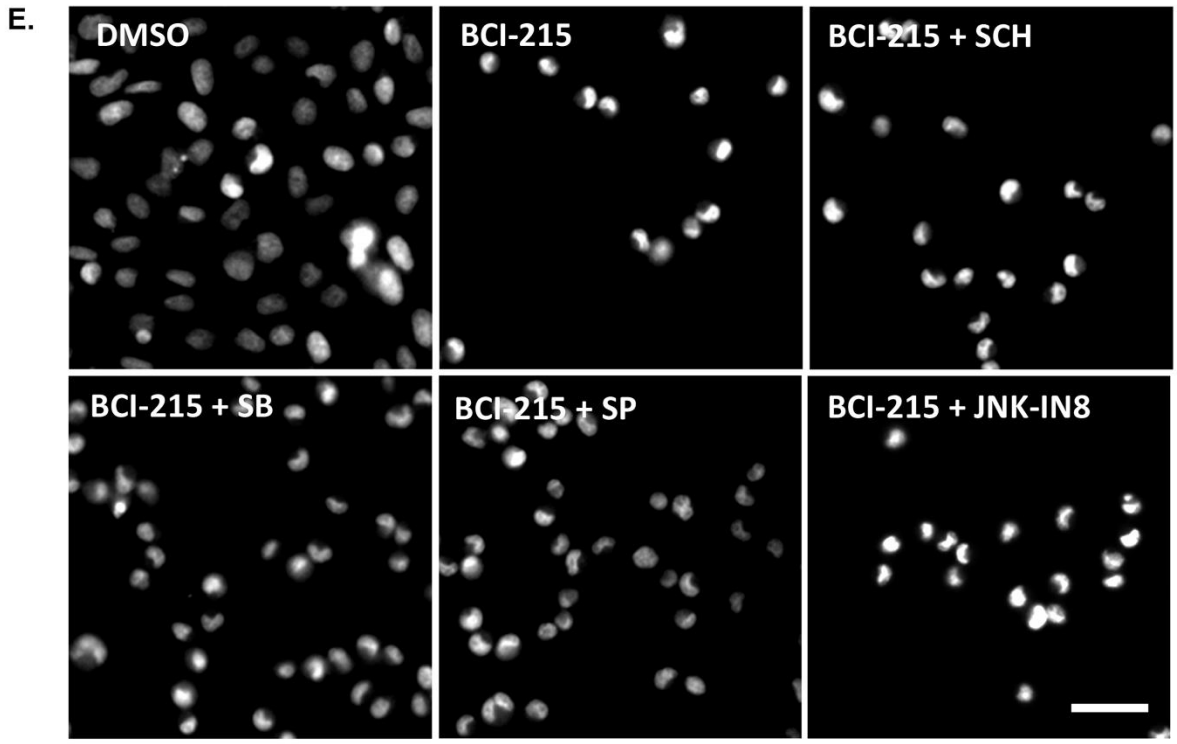

Figure 5

JPET Fast Forward. Published on February 2, 2017 as DOI: 10.1124/jpet.116.239756
This article has not been copyedited and formatted. The final version may differ from this version.

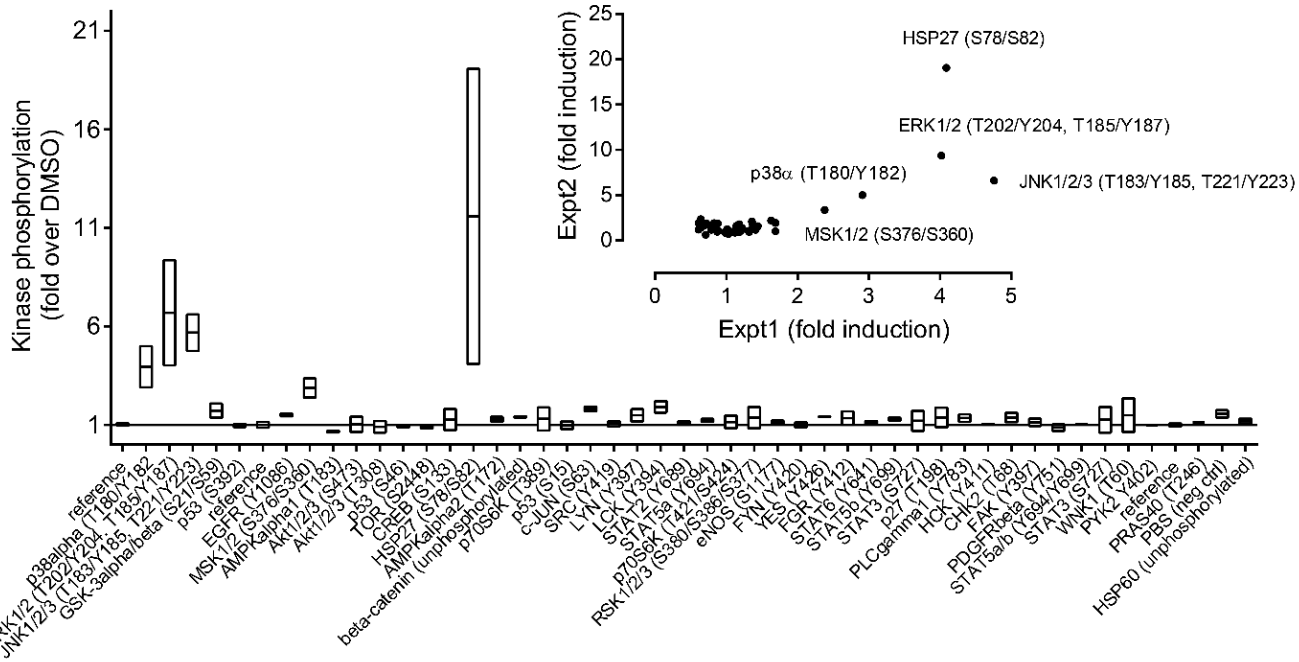

Figure 6

---------- **SUPPLEMENTAL MATERIAL** ----------

A tumor cell-selective inhibitor of mitogen-activated protein kinase phosphatases sensitizes breast cancer cells to lymphokine-activated killer cell activity

Christof T. Kaltenmeier, Laura L. Vollmer, Lawrence Vernetti, Lindsay Caprio, Keanu Davis, Vasiliy N. Korotchenko, Billy W. Day, Michael Tsang, Keren I. Hulkower, Michael T. Lotze, and Andreas Vogt*

Journal of Pharmacology and Experimental Therapeutics

---------- **CONTENTS** ----------

Supplemental Figure 1. Structures of compounds used in this study.

Supplemental Figure 2. Inhibition of motility, survival, and metastatic outgrowth of human breast cancer cells.

Supplemental Figure 3. Fluorescence micrographs of propidium iodide stained MDA-MB-231 cells in 2D and 3D.

Supplemental Table 1. Quantification of multiparametric evaluation of cellular toxicity, caspase-3 activation, and ERK phosphorylation.

SUPPLEMENTARY MATERIALS AND METHODS

HCA of cell motility and cytotoxicity

Colony formation in three dimensional matrigel culture.

Supplemental Figure 1. Structures of compounds used in this study. The study comprises comparative evaluations of three previously described DUSP inhibitors (NSC95397; sanguinarine, (*E*)-2-benzylidene-3-(cyclohexylamino)-2,3-dihydro-1*H*-inden-1-one (BCI), its newly discovered, non-toxic analog (BCI-215), and menadione (vitamin K3) as a positive control for hepatotoxicity). MAPK inhibitors used for pathway evaluation SCH772984, SB203580, SP600125 and JNK-IN-08 were from commercial sources.

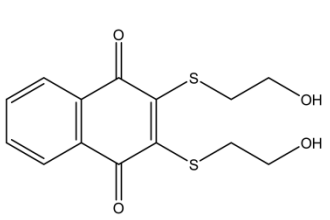

NSC95397

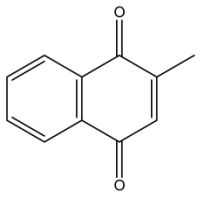

menadione

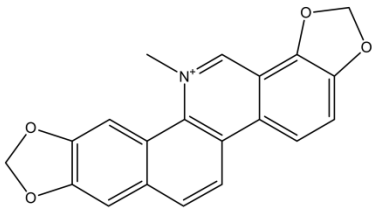

sanguinarine

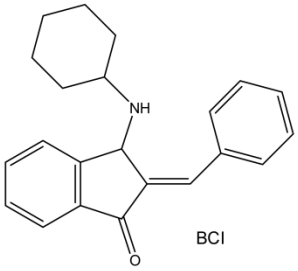

BCI

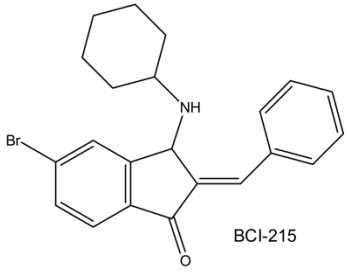

BCI-215

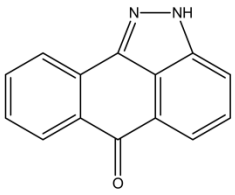

SP600125

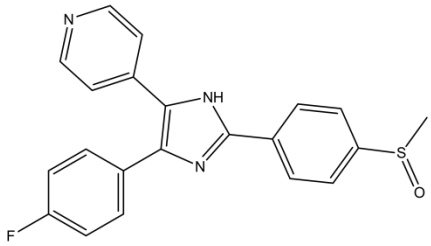

SB203580

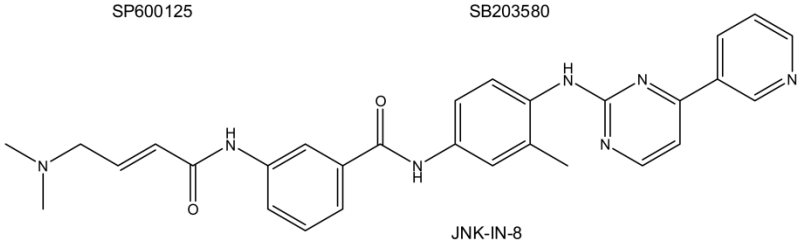

JNK-IN-8

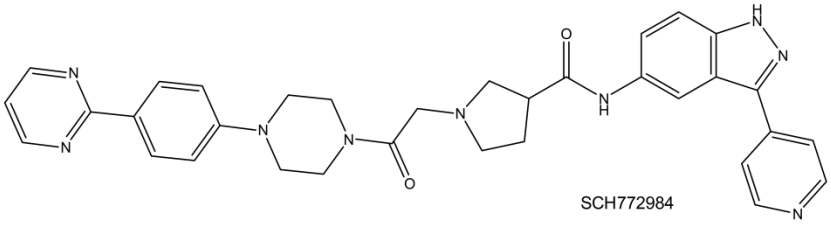

SCH772984

Supplemental Figure 2

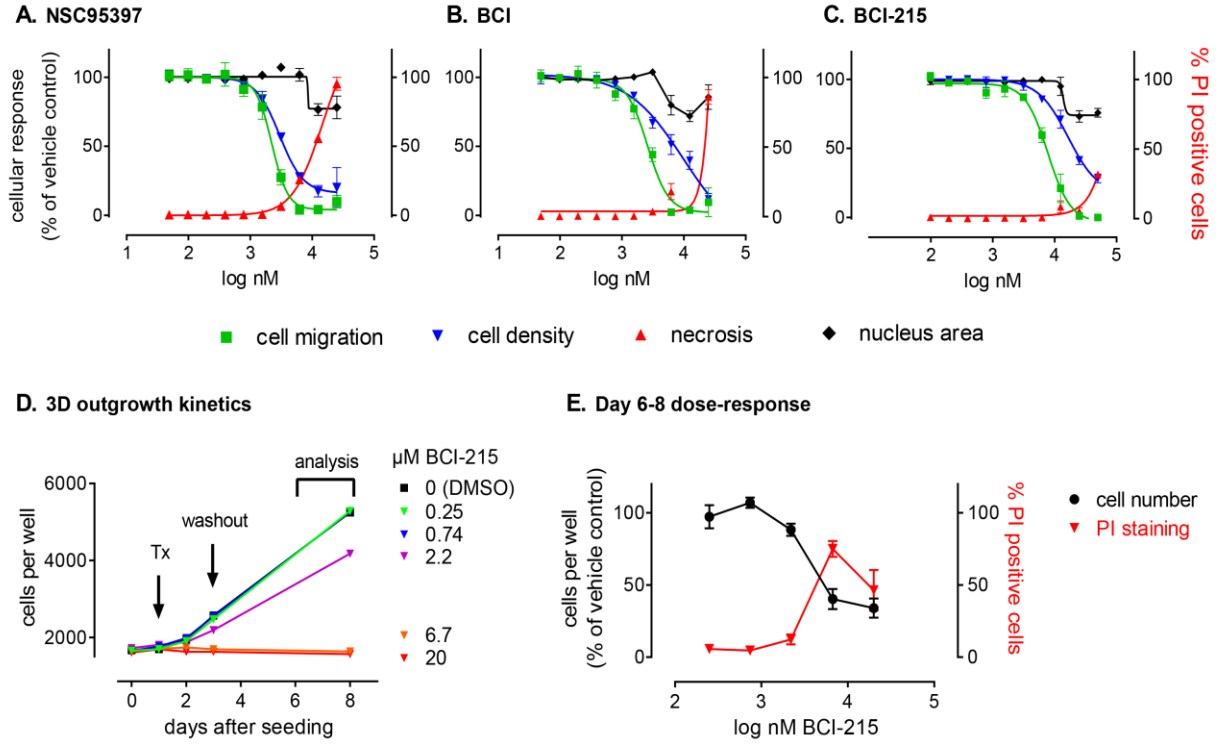

Supplemental Figure 2. BCI-215 inhibits motility, survival, and metastatic outgrowth of human breast cancer cells. (A-C) MDA-MB-231 cells were plated in the wells of an Oris™ Pro 384 cell migration plate, stained with PI and Hoechst 33342 48 h thereafter, and analyzed by high-content analysis for cells that had migrated into the exclusion zone (cell migration), cell loss (cell density), necrosis (% PI positive cells), and nuclear shrinkage (nucleus area). Each data point is the mean of four technical replicates ± SEM from a single experiment that has been repeated four times. All agents inhibited cancer cell migration and caused cell loss with IC50s between 7-15 µM. BCI-215 showed no signs of necrosis at antimigratory and cytotoxic concentrations. **(D)** MDA-MB-231 cells carrying a mitochondrial-targeted, GFP-labeled cytochrome C biosensor were seeded on a layer of matrigel and treated with BCI-215 the next day (Tx). After two days of exposure, drug was washed out and cells allowed to grow for an additional three to five days. Z-stacks were acquired at the indicated time points and cell numbers calculated from maximum projection images. At the end of the study (day 6-8), cells were incubated with PI and the percentage of PI positive cells determined. **(E)** BCI-215 inhibits colony formation and causes pronounced secondary cell lysis in the six-day colony formation assay. Data are the averages ± SEM of three independent experiments, each performed in triplicate.

Supplemental Figure 3. Fluorescence micrographs of propidium iodide stained MDA-MB-231 cells in 2D and 3D.

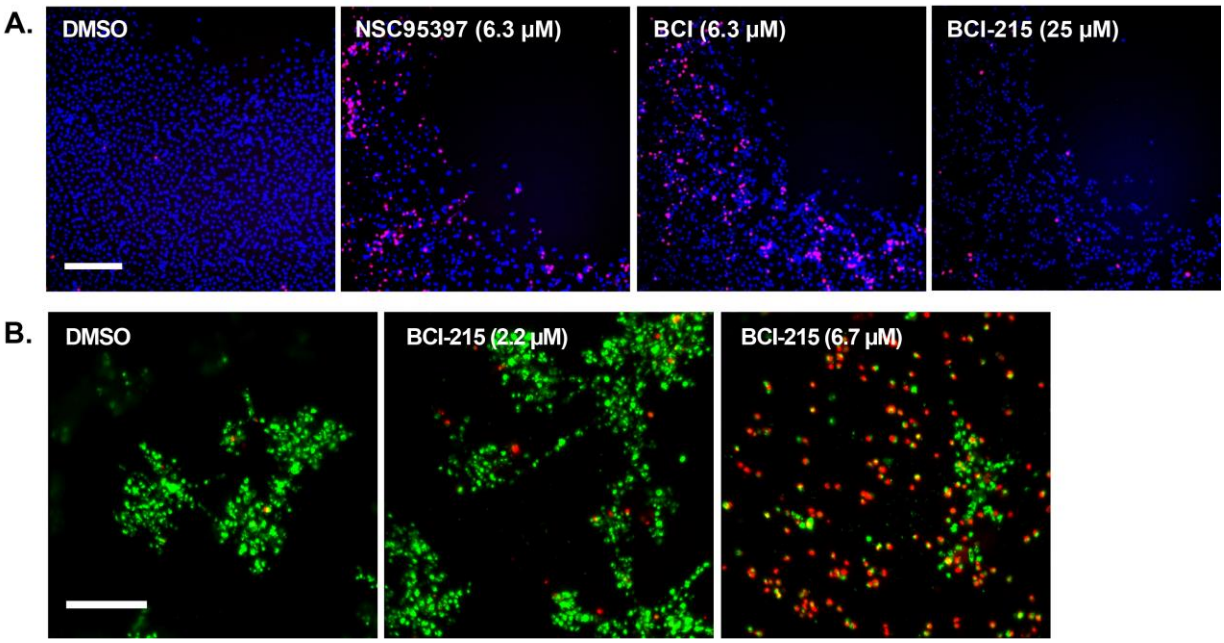

A. Short-term toxicity and motility inhibition on collagen-coated plastic. MDA-MB-231 cells (15,000/well) were plated in the wells of an Oris™ Pro 384 cell migration plate and stained with PI and Hoechst 33342 48 h thereafter. Images show the bottom left quarter of an entire microwell, acquired on the ArrayScan II at 5X, and demonstrate closure of the cell exclusion zone (bare area in the upper right hand corner), cell density (Hoechst stained nuclei in blue), and PI positive cells (red). Scale bar, 300 µm. **B. Toxicity in matrigel six days after treatment with BCI-215.** MDA-MB-231 cells (2000/well) transduced with a biosensor consisting of EGFP with a mitochondrial targeting sequence derived from cytochrome-C oxidase subunit VIII were plated on a cushion of matrigel and treated with vehicle or BCI-215. After two days, medium was replaced and cells allowed to recover for 4 days. Images show GFP/PI overlays of collapsed Z-stacks (20 planes, 5 µm) acquired at 20X magnification on the ImageXpress Ultra. Scale bar, 200 µm.

Supplemental Table 1. Quantification of multiparametric evaluation of cellular toxicity, caspase-3 activation, and ERK phosphorylation.

compound	parameter	IC50 (μM)	SE	95% CI	n
BCI	Nuclear condensation	12.85	1.24	8.261 to 20.00	5
BCI-215	Nuclear condensation	12.77	1.21	8.633 to 18.89	5
BCI	ERK phosphorylation	8.59	1.18	6.137 to 12.03	5
BCI-215	ERK phosphorylation	15.37	1.21	10.35 to 22.81	5
BCI	Caspase-3 cleavage	9.17	1.22	6.019 to 13.97	4
BCI-215	Caspase-3 cleavage	7.33	1.25	4.609 to 11.66	4

Images of pERK stained cells were acquired on the ArrayScan II and analyzed by the Target Activation Bioapplication as described in Materials and Methods. Data are the averages of the indicated numbers of independent experiments, each performed in quadruplicate. For quantification of phospho-ERK and cleaved caspase-3, each well was background corrected by subtracting mean phospho-ERK or cleaved caspase-3 intensities from wells that had received secondary antibody only. IC50, standard error, and 95% confidence intervals were calculated by two way ANOVA with Bonferroni correction in GraphPad Prism.

SUPPLEMENTARY MATERIALS AND METHODS

HCA of cell motility and cytotoxicity was performed essentially as described (1). MDA-MB-231 cells (15,000/well) were plated in collagen-coated Oris™ Pro 384-well microplates (Platypus Technologies cat # PRO384CMACC5) containing a chemical exclusion zone that dissolves upon cell seeding. Two hours after plating, medium was removed, and cells treated with ten-point, two-fold concentration gradients of test agents. Forty-eight hours after treatment, cells were stained with 10 µg/ml Hoechst 33342 and 1 µg/ml PI in HBSS for 15 min at 37°C. Plates were washed once with PBS and scanned live on the ArrayScan II using a 5X objective. To capture cells that had entered into the exclusion zone, a single field was acquired in the center of the well and nuclei therein enumerated. To assess changes in cell loss, nuclear size, and necrotic cell death, a second scan was performed that captured one field at the edge of the well (see (1) for more detail). Parameters exported and plotted were SelectedObjectCountPerValidField (cell density), MEAN_ObjectAreaCh1 (nucleus size), and %RESPONDER_MeanAvgIntenCh2 (percent PI positive cells based on based on a threshold set with vehicle treated cells).

Colony formation in three dimensional matrigel culture. MDA-MB-231 cells (2000/well) transduced with a biosensor consisting of EGFP with a mitochondrial targeting sequence derived from cytochrome-C oxidase subunit VIII (2) were trypsinized, resuspended in RPMI1640 containing 2% FBS and 2% matrigel, and seeded in 384 well microplates on a 15 µl cushion of undiluted matrigel. After 24 hours, cells were treated with various concentrations of BCI-215 or vehicle (0.2% DMSO). After two days, drug was washed out and cells allowed to expand for an additional three to five days. At the end of the study, medium was replaced with HBSS containing 4 µg/ml PI for 1 hour, and plates scanned live on an ImageXpress Ultra HCS reader, acquiring z-stacks (4X objective, 20 planes, 50 µm) in the green and red

channels. Cell numbers were quantified from maximum projection images using the Multiwavelength Cell Scoring application.

REFERENCES

1. Joy ME, Vollmer LL, Hulkower K, Stern AM, Peterson CK, Boltz RC, et al. A high-content, multiplexed screen in human breast cancer cells identifies profilin-1 inducers with anti-migratory activities. PLoS One. 2014;9:e88350.

2. Senutovitch N, Vernetti L, Boltz R, DeBiasio R, Gough A, Taylor DL. Fluorescent protein biosensors applied to microphysiological systems. Exp Biol Med (Maywood). 2015;240:795-808.